IEEE Access
Multidisciplinary : Rapid Review : Open Access Journal

Received 23 February 2023, accepted 13 March 2023, date of publication 16 March 2023, date of current version 22 March 2023.

Digital Object Identifier 10.1109/ACCESS.2023.3257985

RESEARCH ARTICLE

Miniaturized Power Divider With Triple-Band Filtering Response Using Coupled Line

DILIP KUMAR CHOUDHARY [1], (Senior Member, IEEE), **NAVEEN MISHRA** [1], **PRASHANT KUMAR SINGH** [2], AND **ANAND SHARMA** [3], (Member, IEEE)

[1]School of Electronics Engineering, Vellore Institute of Technology, Vellore 632014, India
[2]Department of Electronics and Communication Engineering, Birsa Institute of Technology Sindri, Dhanbad, Jharkhand 828123, India
[3]Department of Electronics and Communication Engineering, Motilal Nehru National Institute of Technology Allahabad, Prayagraj 211004, India

Corresponding author: Dilip Kumar Choudhary (dilip.choudhary6@gmail.com)

ABSTRACT This proposed work describes a miniaturized and simple power divider that uses coupled lines for a triple-band filtering response. The intended setup includes an isolation resistor connecting the output feed lines through Structure-3 and coupled line-based microstrip resonators connected to the input feed line. The presented power divider achieves three passbands with a filtering response. The first and second passbands are achieved by the coupled line structure that includes Resonator-1 and Resonator-2. The third passband is realized due to Resonator-3. Furthermore, by varying the structural parameter of the designed triple-band filtering power divider, the resonance frequencies of all three passbands can be controlled because of changes in their equivalent lumped parameters. The resonance frequency mainly depends on its equivalent inductance and capacitance value. For validation of the simulation result, the filtering power divider structure has been fabricated and tested. The experimental results denote that the prototype has a fractional bandwidth (|S21| <-3 dB) of about 20.0 % (1.1 GHz to 1.35 GHz), 37.0 % (2.0 GHz to 2.9 GHz), and 15.0 % (3.25 GHz to 3.8 GHz) respectively for first, second and third passbands respectively. This arrangement shows isolation above 18 dB for all three bands with a downsized of $0.10\lambda_g \times 0.12\lambda_g$ (25 mm×30 mm) according to the operating frequency of the first frequency passband. The triple band performance of the developed component shows a good input reflection coefficient. The operating frequencies, which are suitable for the application of the *L*-band, WLAN, sub-6 GHz band of 5G, include 1.23 GHz, 2.41 GHz, and 3.55 GHz.

INDEX TERMS Coupled line, isolation, filtering power divider, miniaturized, triple-band.

I. INTRODUCTION

Due to its ability to both filter and distribute power, the microwave filtering power divider (FPD) has attracted a lot of attention from the wireless communication research community in recent years [1], [2]. In a Wilkinson power divider (WPD), a passband filter structure was used in place of a quarter-wave transmission line (QTL) to get both the power division response and filter response [3], [4], [5]. There have been several high-performing single passband FPDs grounded on WPD structure, substrate-integrated waveguide (SIW) configuration, and dual-composite right-left handed (D-CRLH) structure that has been studied in the past [6], [7], [8]. A bandpass along with two lowpass filters has been replaced with conventional WPD to attain filtering behaviour [6]. A SIW-based power divider with bandpass performance is presented in [7] by incorporating a metamaterial structure. It includes an interdigital capacitor between two complementary split-ring resonators. To produce the miniaturized FPD, a band-pass filter (BPF) using a D-CRLH structure was replaced with QTL in a WPD [8]. Due to the rising need for multi-frequency modern wireless technologies, the requirement for multiband FPDs is of the highest importance at the moment. The literature has various dual-band FPDs [9], [10], [11], however, research on triple-band FPDs [12], [13], [14], [15] is still in its infancy.

A dual-band performing FPD for satellite communication is examined in [9] employing via-less D-CRLH resonators.

The associate editor coordinating the review of this manuscript and approving it for publication was Wenjie Feng.

It offers a ninety-degree phase delay for lower frequency and phase advance for higher frequency. Gysel Power Divider [10] is recommended to utilize two phase shifters in order to simultaneously produce two passbands. The frequency bands in this case are controlled by the transmission cables' impedance. The dual-band FPD configuration consists slotted defected ground structure along with a T-shaped stub structure at the upper side of the substrate [11]. In this more transmission zeros are generated with the help of more resistors connected between output ports. In [12] presents a triple band FPD that combines a quasi WPD and a shorted stepped impedance resonator (SIR). The impedance ratio of the SIR controls the two frequencies (lower and higher), while a half-wavelength resonator tunes the middle frequency. Utilizing fork-shaped type triple mode resonators [13], connected through input/output lines, the tri-band FPD structure has been investigated. By placing two resistors between two pairs of symmetrical resonators centred on the central input feed line, the isolation between the ports is also increased. Designing a triple band filtering power divider with stepped resonators using signal interference techniques is also suggested [14]. In [15], a triple-band FPD has been reported with coupled microstrip line consisting of two bandstop resonators and one passband resonator.

This study discusses a revolutionary coupled lines-based triple band filtering power divider (FPD) and its thorough design process. The three passband zones are represented by the proposed FPD as 1.10 to 1.35 GHz, 2.0 to 2.9 GHz, and 3.25 to 3.8 GHz. Correct loading of the isolation resistor between the output lines results in the desired isolation within the three passbands. The structure's electrical trace, which measures $0.10\lambda_g \times 0.12\lambda_g$, serves as an example of how compact it is. Here wavelength (λ_g) is concerning a lower operating frequency of 1.23 GHz. It is appropriate for 5G sub-6 GHz, WLAN, and L-band applications. A miniaturized and simple triple-band FPD based on coupled lines for multiband wireless application is presented in this work.

II. CONFIGURATION AND DESIGN

This section describes the structure configuration and design of the triple-band bandpass filter and triple-band filtering power divider.

A. TRIPLE BAND BANDPASS FILTER

The triple-band BPF is composed of coupled line resonators named Resonator-1, Resonator-2 and Resonator-3, respectively as mentioned in its layout diagram. The layout of the designed triple-band BPF has illustrated in revised Fig. 1(a) and the developing stage of the triple band with its scattering parameters are shown in Fig 1(b). The first passband is mainly achieved due to Resonator-1, which consists rectangular patch connected with feedline port-1 and port-2 with the help of a strip line. Due to the rectangular patch and stripline, some amount of inductance is generated and due to the gap between the patch and port-2, some amount of capacitance is generated. And the combined effect of these lumped elements

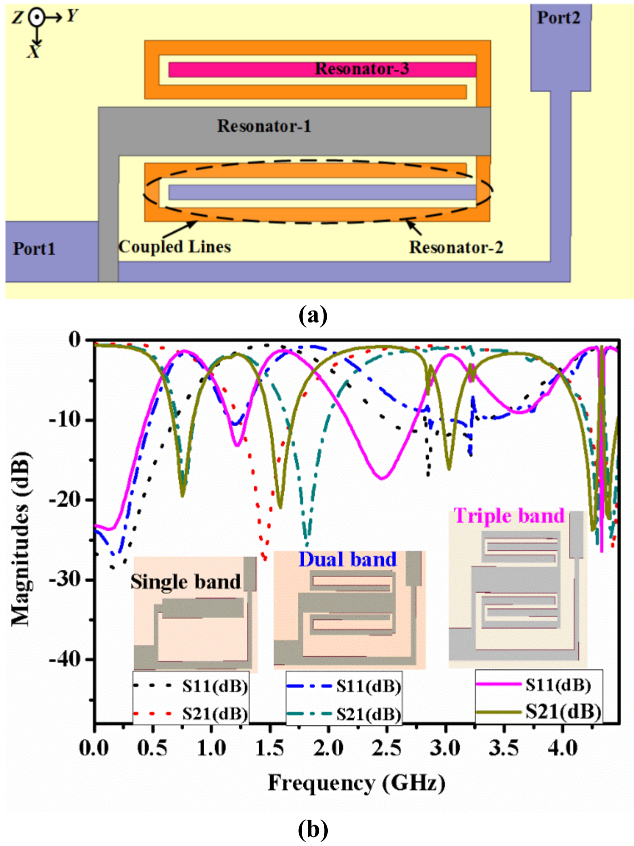

FIGURE 1. Designed triple-band BPF (a) Layout (b) Developing stage of the triple-band filer.

resonates at 3.0 GHz, but with poor impedance matching and selectivity. Further, a coupled line named Resonator-2 connected with resonator-1. Due to the combined effect of both resonators dual passband response has been achieved with the operating frequency of 1.2 GHz and 3.0 GHz. The proposed triple-band bandpass filter has been achieved due to a combination of all three resonators. Inside the Resonator-2, a strip line named Resonator-3 was inserted Resonator-2, which produces some extra amount of lumped elements inductance and capacitance. Due to the combined effect of all resonators triple-pass band response was achieved which resonates at 1.2 GHz, 2.4 GHz and 3.5 GHz, respectively.

B. TRIPLE BAND FILTERING POWER DIVIDER

The structural outline of the intended power divider is demonstrated in Fig. 2. The impedance transformation structure named Structure-1, and Structure-2 for tri-bandpass filters and the transmission line named Structure-3 that connects input-output ports with the same characteristics impedance are utilized for designing of FPD structure. The two tri-band passband filters were embedded in two symmetric branches of the power divider distinctly. The design equation of the Wilkinson power divider [4] can be written as

$$R = Z_1 \left((k^2 + 1) \middle/ k \right) \tag{1}$$

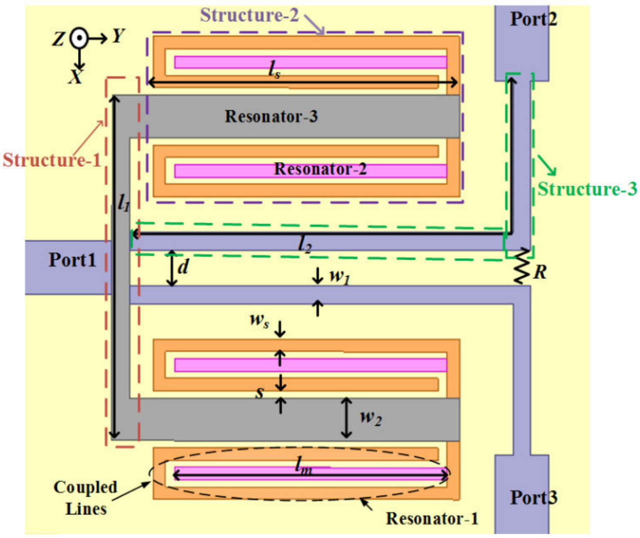

FIGURE 2. The structural layout of the designed triple band filtering power divider [All dimensions are in mm: $l_1 = 19.5$, $l_2 = 31.0$, $l_s = 17.2$, $l_m = 15.3$, $w_1 = 1.0$, $s = 0.4$, $w_s = 0.7$, $w_2 = 2.4$, $d = 2.0$].

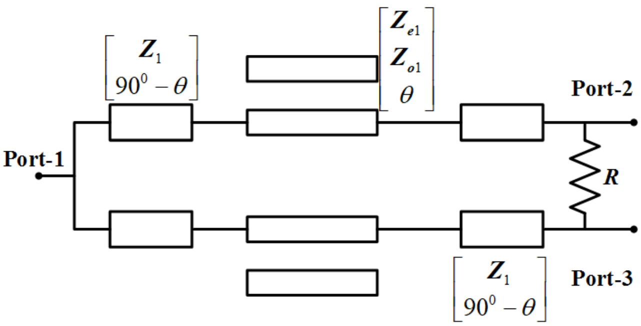

FIGURE 3. Configuration of proposed triple-band FPD.

Here, Z_1 represents source/load impedance, k^2represents the power ratio and R is the isolation resistance between output ports (port-2 and port-3) respectively. Therefore for the proposed structure $R = 2Z_1$.

The configuration of the proposed design comprising four design parameters as impedances Z_1, Z_{e1}, Z_{01} and electrical length θ, are illustrated in Fig. 3. We utilize odd and even mode decomposition method to study power divider because of its symmetry. The equivalent even and odd circuit model is depicted in Fig. 4. It predicts its equivalent even and odd mode circuit and its equivalent to the inverter circuit. The designed structure is a triple-band first-order FPD. Its impedance value can be derived as [4], [5], [13], [16], and [17] in terms of admittance inverter (J) and susceptance (B). If we assume fractional bandwidth (Δ) and elemental value g_1 and g_2, then the electrical length θ will be:

$$\theta = 90^o \frac{2\sqrt{g_1 g_2}}{2\sqrt{g_1 g_2 + \Delta}} \tag{2}$$

$$\text{Susceptance}, B = 2b\frac{f - f_o}{f_o} - \frac{J^2}{2b}\frac{f_o}{f - f_o} \tag{3}$$

$$\text{Admittance inverter}, J = \sqrt{\frac{\Delta b}{Z_1 g_1 g_2}} \tag{4}$$

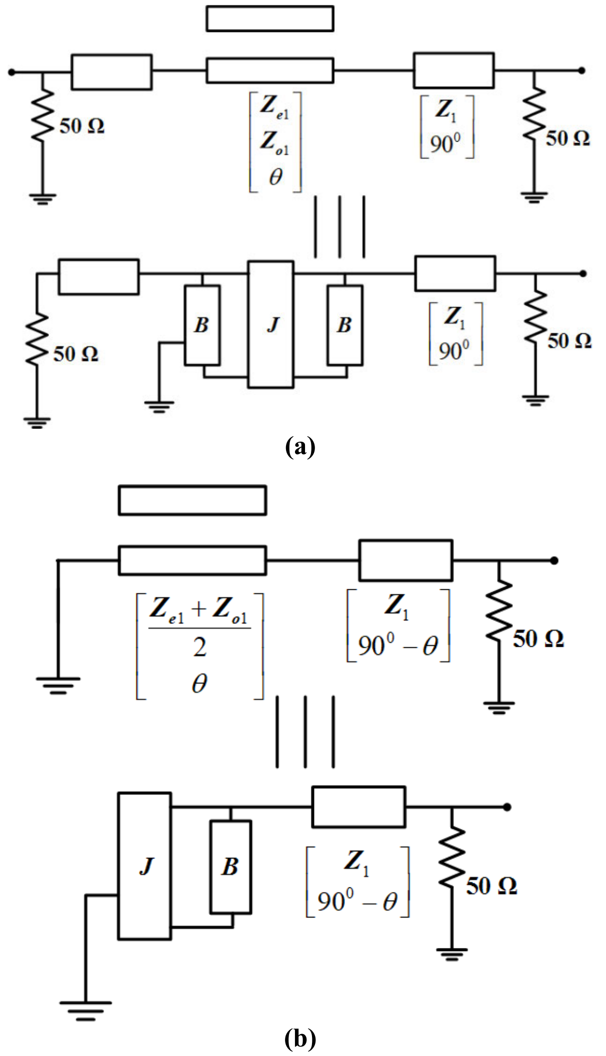

FIGURE 4. Presented equivalent circuit of triple-band FPD (a) Even mode configuration. (b) Odd mode configuration.

$$\text{Even impedance}, Z_{e1} = Z_1\frac{1 + JZ_1 \csc\theta + J^2 Z_1^2}{1 - J^2 Z_1^2 \cot^2\theta} \tag{5}$$

$$\text{Odd impedance}, Z_{o1} = Z_1\frac{1 - JZ_1 \csc\theta + J^2 Z_1^2}{1 - J^2 Z_1^2 \cot^2\theta} \tag{6}$$

where 'b' represents the slope parameter whose value is nearly equal to $\pi/4Z_1$, and the centre frequency is represented by f_o. The resonance frequency can be calculated by equating the susceptance value equal to zero and by setting Z_{e1}, and Z_{01} to zero. The resonance frequency be

$$f_{r1} = f_o\left(1 - \frac{J}{2b}\right), \quad f_{r2} = f_o\left(1 + \frac{J}{2b}\right), f_{r3} = \frac{\pi f_o}{2\theta}.$$

The transmission zero can be calculated by equating Z_{e1} to Z_{01}.

Fig. 5(a) demonstrates the structural schematic topology of the proposed triple-band filtering power divider. The dashed circle represents by exchange of the quarter wavelength of the conventional Wilkinson power divider with the BPF filtering power divider achieved. The BPF filter is composed of a triple

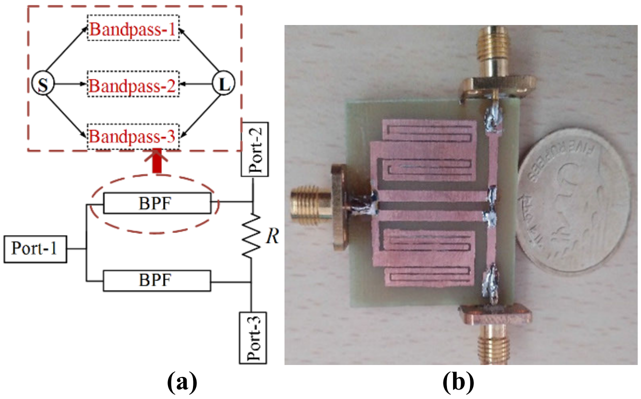

FIGURE 5. Proposed filtering power divider: (a) Schematic topology, (b) fabricated prototype.

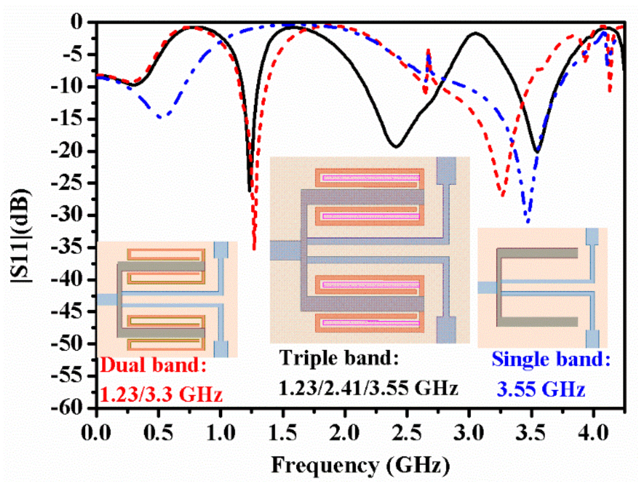

FIGURE 6. Developing stage of the filtering power divider.

passband structure, in which the first passband is achieved due to Resonator-1. The second and third pass-bands initiate mainly because of Resonator-2 and Resonator-3, respectively. Then, among the terminating ends Structure-3, an isolation resistor R is employed to achieve adequate isolation between port-2 and port-3. By adjusting the impedance ratio and electrical length of the designed structure, three desirable passbands can be obtained instantaneously. The designed FPD fabricated model has illustrated in Fig. 5(b). The developing steps of the designed tri-band FPD have illustrated in Fig.6. Because of Resonator-3, one band appears at 3.55 GHz. The second band at 1.23 GHz mainly appears due to resonator-1. Between these two passbands, a third band appears because of resonator-2, which resonates at 2.41 GHz.

III. ANALYSIS OF FPD

Low-cost FR4 with a dielectric constant, loss tangent and thickness of 4.4, 0.029, and 1.6 mm is the substrate utilized to design the suggested FPD structure. The simulation and measured S-parameter of the designed tri-band FPD illustrated in Fig. 7, shows reasonable agreement. Figure 7(a) displays the frequency-dependent insertion loss (|S21|), return loss (|S11|), and both (|S31|) in the dB. In this design, the operating bandwidth is defined as the passband width

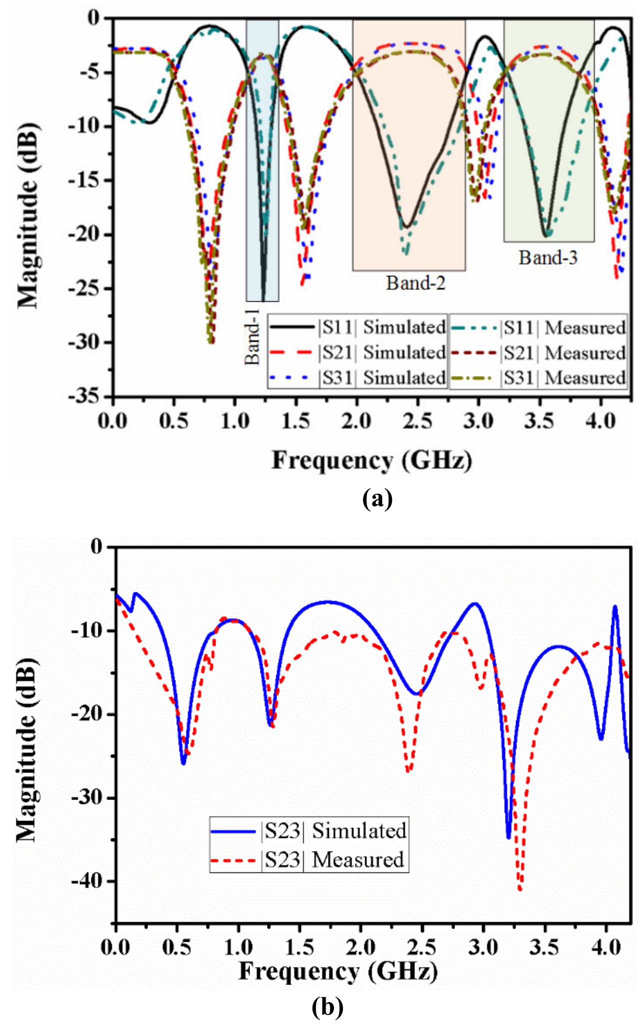

FIGURE 7. Simulated and measured S-parameter of fabricated tri-band FPD indicated by (a) |S11|, |S21| and |S31|, and (b) isolation |S23|.

|S21| = |S31| <3dB. About 20.0% (1.1 to 1.35 GHz), 37% (2.0 to 2.9 GHz), and 15% (3.25 to 3.8 GHz) are the 3-dB fractional bandwidths (3.25 GHz –3.8 GHz). The planned structure operates at frequencies of 1.23 GHz, 2.41 GHz, and 3.55 GHz. Return losses in the three passband regions that correspond to them are 26.0 dB, 19.5 dB, and 20.0 dB, respectively. After subtracting 3 dB, the insertion losses in each band of the FPD are calculated to be 1.0 dB, 0.2 dB, and 0.2 dB. The simulated isolation of all three frequency bands is more than 23, 18, and 35 dB, respectively, as depicted in Fig. 7(b). Additionally, all three passbands' in-band isolation is better than 13.5 dB.

The intended operating frequencies can be achieved or disciplined by changing the structural parameters as presented in Fig. 8. The working frequencies of the FPD vary as the length "*ls*" varies, as seen in Fig. 8(a). The proposed FPD's operating frequency is controlled by changes in the coupled line's length (*ls*), as longer coupled lines have more inductance, which lowers the resonant frequency. While varying the length of coupled line (*ls*), when the length of *ls* increases, the equivalent amount of inductance increases, so all the

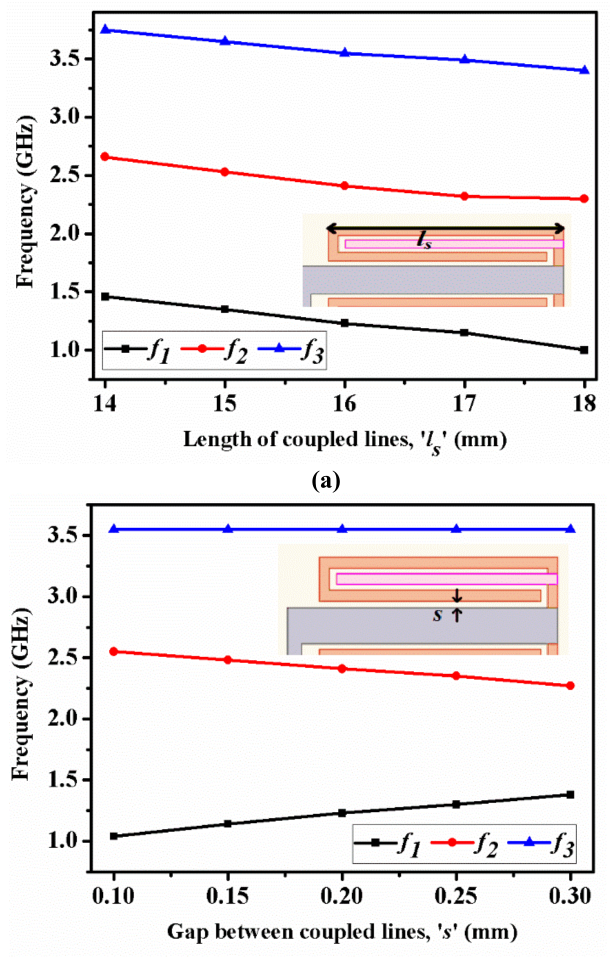

FIGURE 8. Deviation in working frequency because of change in (a) in the length (ls) of coupled line, and (b) change in the gap (s) between coupled lines.

resonating frequency decreases. This follows the basic resonating frequency, $f_0 = \frac{1}{2\pi\sqrt{LC}}$, as we increase the value of Inductance the resonating frequency shifts toward a lower value. Fig. 8 (b) depicts the relationship between the operating frequencies and the gap (s) between Resonator-2 and Resonator-3. While changing the separation (s) between Resonator-2 and 3, the first and second resonating frequencies (f_1 and f_2) will vary but the third resonating frequency (f_3) remains constant. The first resonating frequency does not depend on gap 's'.

By selecting the appropriate chip resistor value, as displayed in Fig. 9, the isolation of the suggested triple-band FPD can be increased. This demonstrates that the isolation between the output feed lines is improved by increasing the resistance, or 'R', that connects them. The formation of the various passbands is confirmed by the examination of the electric field distributions for the suggested arrangement. The tri-band FPD structure's E-field at its operating frequencies is shown in Fig. 10. According to Fig. 10, the linked line resonators' upper and lower sections are where the concentrated E-field is established at 1.23 GHz (a). The central region of the connected line resonators is where the E-field concentration is seen for 2.41 GHz operation, as displayed in Fig. 10. (b). However, Fig. 10(c) reveals that the linked line resonator's midsection and the output ports, Port-2 and Port-3, are where the largest E-field is concentrated.

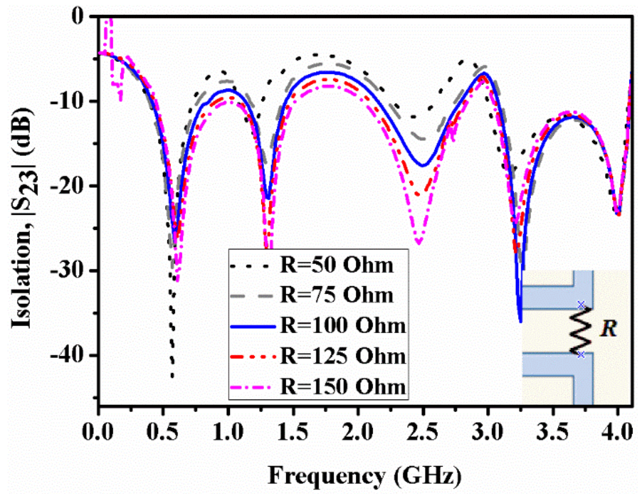

FIGURE 9. Isolation versus resistance plot of designed tri-band FPD.

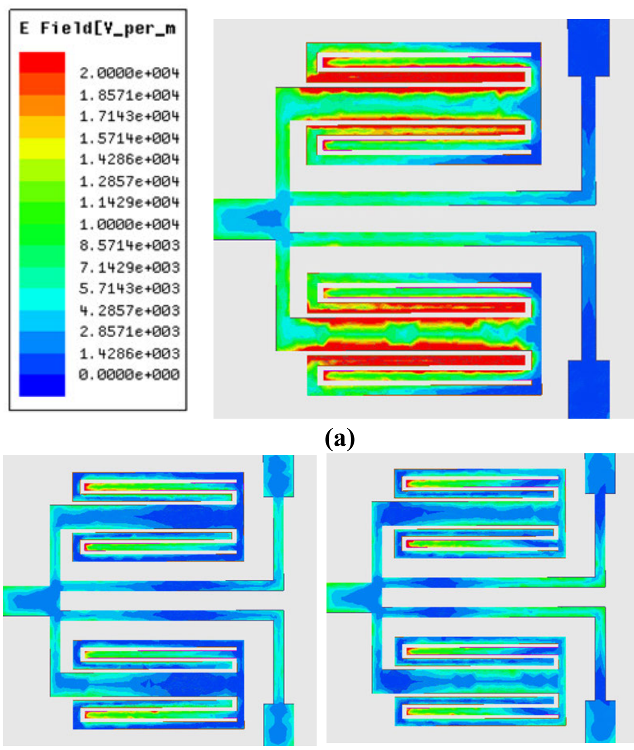

FIGURE 10. E-field distribution of presented tri-band FPD: (a) 1.23 GHz, (b) 2.41 GHz, and (c) 3.55 GHz.

The lumped equivalent circuit model of the designed triple band filtering power divider has been shown in Fig.11. In the equivalent circuit because of structure-1 as mentioned in Fig. 2 of the manuscript, the inductance L_1appears. Due to structure-2, the inductance L_2 and L_3 appear which is connected between input and output ports. The inductance

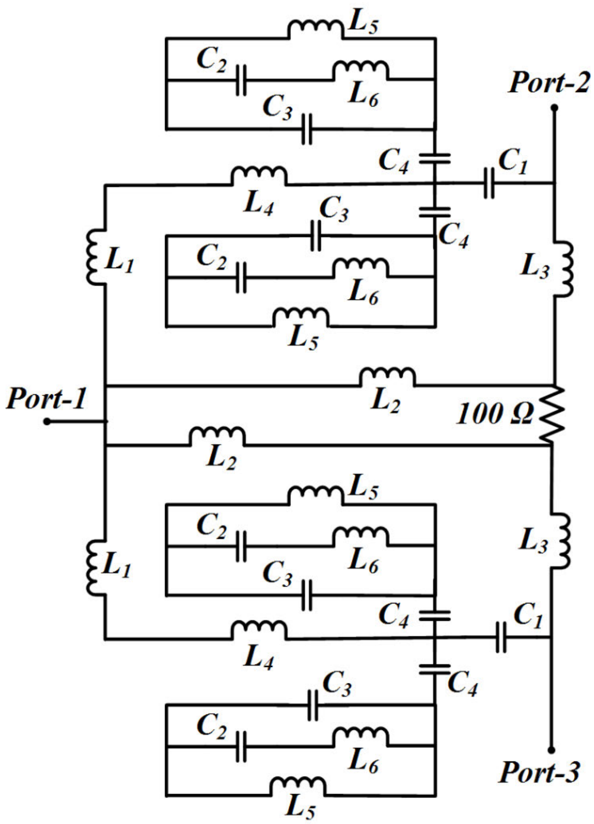

FIGURE 11. Lumped Equivalent Circuit model of proposed triple-band FPD.

L_4 appears mainly because of Resonator-3 and due to the gap between Resonator-3 and Structure-2 the capacitance C_1 will appear. The parallel combination of Inductance L_5 and capacitance C_3 is generated due to coupled line Resonator-1. The series combination of inductance L_6 and capacitance C_2 appears between parallel combinations of L_5C_3 because of Resonator-2. Due to the gap between Resonator-2 and Resonator-3 the coupling capacitance C_4 appears. The isolation resistance of value *100* ohms is connected between two output ports named Port-2 and Port-3. This equivalent lumped circuit model has been designed on circuit-simulated software ADS. The values of lumped equivalent circuit model are as follows: $L_1 = 16.5$ nH, $L_2 = 66.1$ nH, $L_3 = 5.1$ nH, $L_4 = 10.2$ nH, $L_5 = 0.63$ nH, $L_6 = 33.7$ nH, $C_1 = 0.85$ pF, $C_2 = 3.11$ pF, $C_3 = 4.64$ pF, and $C_4 = 30.07$ pF. The scattering parameters of the designed equivalent circuit model has illustrated in Fig.12. Which shows the return loss (|S11|) of the designed triple band filtering power divider. We can control the resonance frequency of all three pass bands by varying the lumped circuit values.

Table 1 compares the planned study with other tri-band FPDs that have been reported in the introduction and are available in the literature. Operating frequencies, Insertion loss, Return loss, in-band isolation, and electrical size are some of the performance metrics listed in the table. The suggested tri-band FPD is suitable for wireless systems due to its small size, high isolation, and effective filtering.

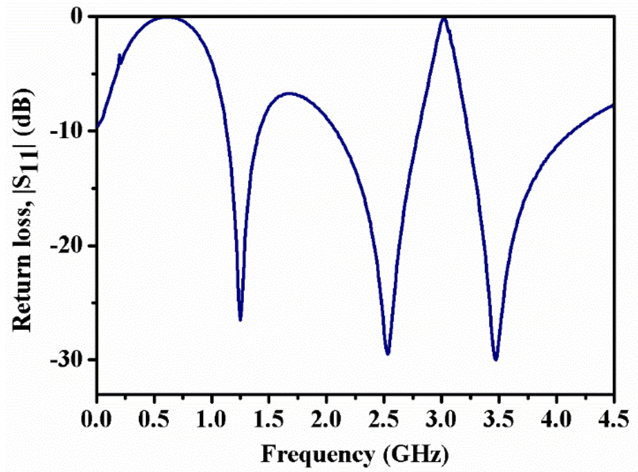

FIGURE 12. Scattering parameters of a lumped circuit model of designed triple band FPD.

TABLE 1. Comparison between proposed work and previous work.

Ref.	Frequency (GHz)	In-band Isolation (dB)	Insertion loss (dB)	Return loss (dB)	Electrical Size ($\lambda_g \times \lambda_g$)
[10]	3.49/4.13/5.57	>14.2	1.15/1.18/1.5	25.1/19.6/28	0.28 × 0.28
[11]	1.52/2.0/2.36	>15.0	2.322/1.2/2.8	15.4/19.1/17.3	0.69 × 0.36
[12]	2.4/4.4/6.1	>12.0	3.1/3.13/3.28	>15.0	0.38 × 0.42
[13]	2.32/2.4/2.51	>19.0	12.9/2.2/1.98	>17.0	--
This work	1.23/2.41/3.55	>18.0	1.0/0.2/0.2	26.0/19.5/20	0.10 × 0.12

IV. CONCLUSION

This work presents a miniaturized triple-band filtering power divider with operating frequencies of 1.23 GHz, 2.41 GHz, and 3.55 GHz based on microstrip coupled line resonators. In multiband wireless communication protocols like L-band, Wi-Fi, and sub-6 GHz of 5G technology, this illustrates how the proposed design can be used. With in-band isolation better than 18 dB, the operational band's transmission and reflection coefficients are observed to be below 1 dB and above 19.5 dB, respectively. By connecting an isolation resistor between the output feed lines, good isolation is made possible. The linked line resonators are used to achieve compactness. The operating frequencies, which are suitable for *L*-band, WLAN, and sub-6 GHz band of 5G applications, include 1.23 GHz, 2.41 GHz, and 3.55 GHz.

REFERENCES

[1] Y. Deng, J. Wang, L. Zhu, and W. Wu, "Filtering power divider with good isolation performance and harmonic suppression," *IEEE Microw. Wireless Compon. Lett.*, vol. 26, no. 12, pp. 984–986, Dec. 2016.

[2] D. K. Choudhary and R. K. Chaudhary, "A compact SIW based filtering power divider with improved selectivity using CSRR," in *Proc. Prog. Electromagn. Res. Symp.*, Singapore, Nov. 2017, pp. 1334–1337.

[3] C.-F. Chen, T.-Y. Huang, T.-M. Shen, and R.-B. Wu, "Design of miniaturized filtering power dividers for system-in-a-package," *IEEE Compon., Packag., Manuf. Technol.*, vol. 3, no. 10, pp. 1663–1672, Oct. 2013.

[4] D. M. Pozar, *Microwave Engineering*, 4th ed. New York, NY, USA: Wiley, 2012.

[5] J. S. Hong and M. J. Lancaster, *Microstrip Filters for RF/Microwave Applications*, 2nd ed. Hoboken, NJ, USA: Wiley, 2011.
[6] W.-M. Chau, K.-W. Hsu, and W.-H. Tu, ''Filter-based Wilkinson power divider,'' *IEEE Microw. Wireless Compon. Lett.*, vol. 24, no. 4, pp. 239–241, Apr. 2014.
[7] H. Chen, W. Che, X. Wang, and W. Feng, ''Size-reduced planar and nonplanar SIW Gysel power divider based on low temperature co-fired ceramic technology,'' *IEEE Microw. Wireless Compon. Lett.*, vol. 27, no. 12, pp. 1065–1067, Dec. 2017.
[8] D. K. Choudhary and R. K. Chaudhary, ''Compact D-CRLH structure for filtering power divider,'' *Prog. Electromagn. Res. Lett.*, vol. 94, pp. 93–101, 2020.
[9] T. Huang, L. Feng, L. Geng, H. Liu, S. Y. Zheng, S. Ye, L. Zhang, and H. Xu, ''Compact dual-band Wilkinson power divider design using via-free D-CRLH resonators for Beidou navigation satellite system,'' *IEEE Trans. Circuits Syst. II, Exp. Briefs*, vol. 69, no. 1, pp. 65–69, Jan. 2022.
[10] C.-W. Tang and Z.-Q. Hsieh, ''Design of a planar dual-band power divider with arbitrary power division and a wide isolated frequency band,'' *IEEE Trans. Microw. Theory Techn.*, vol. 64, no. 2, pp. 486–492, Feb. 2016.
[11] Y. Rao, H. J. Qian, B. Yang, R. Gomez-Garcia, and X. Luo, ''Dual-band bandpass filter and filtering power divider with ultra-wide upper stopband using hybrid Microstrip/DGS dual-resonance cells,'' *IEEE Access*, vol. 8, pp. 23624–23637, 2020.
[12] K. Song, M. Fan, F. Zhang, Y. Zhu, and Y. Fan, ''Compact triple-band power divider integrated bandpass-filtering response using short-circuited SIRs,'' *IEEE Trans. Compon., Packag., Manuf. Technol.*, vol. 7, no. 7, pp. 1144–1150, Jul. 2017.
[13] G. Zhang, X. Zhang, S. Liu, L. Tang, J. Yang, and J. Hong, ''Tri-band filtering power divider based on multi-mode fork-type resonator for performance enhancement,'' *IET Microw., Antennas Propag.*, vol. 14, no. 9, pp. 867–873, Jul. 2020.
[14] C. Liu, M. Wu, J. Yuan, K. L. Chung, and Y. Li, ''A tri-band Wilkinson power divider based on triple section step-impedance resonator, in *Proc. IEEE 3rd Int. Conf. Electronic Inf. Commun. Technol. (ICEICT)*, Shenzhen, China, Nov. 2020, pp. 765–767.
[15] Z. Zhang, G. Zhang, R. Li, S. Zhang, Q. Chen, L. Chen, Z. Yang, and W. Tang, ''A simple triple-band coupled line filtering power divider design,'' *Microw. Opt. Technol. Lett.*, vol. 64, no. 1, pp. 5–9, Jan. 2022.
[16] C. J. Chen, ''Design of parallel coupled dual mode resonator bandpass filter,'' *IEEE Trans. Compon., Packag., Manuf. Technol.*, vol. 6, no. 10, pp. 1542–1548, Oct. 2016.
[17] C.-J. Chen and Z.-C. Ho, ''Design equations for a coupled-line type filtering power divider,'' *IEEE Microw. Wireless Compon. Lett.*, vol. 27, no. 3, pp. 257–259, Mar. 2017.

DILIP KUMAR CHOUDHARY (Senior Member, IEEE) received the Ph.D. degree in electronics engineering from the Indian Institute of Technology (ISM) Dhanbad, India, in 2020. He is currently an Assistant Professor with the School of Electronics Engineering, Vellore Institute of Technology, Vellore, India. His main areas include the electromagnetic simulation and characterization of microwave filtering circuits using metamaterial structures for wireless communication. He has authored more than 34 referred journals and conference papers, including 16 SCI journals. He has authored one copyright and three book chapters. His current research interests include microwave filtering circuits, metamaterial and their applications, microwave filters, antennas, MIMO antennas, absorbers, power dividers, and couplers for wireless communication. He is a Senior Member of MTT, APS, and the AESS Society. He was a recipient of the International Travel Grant from DST, India, in 2017, and the Best Paper award at PIERS, Singapore, in 2017. He served as the Session Chair ''Poster Session 2-P'' at the 2017 IEEE Asia Pacific Microwave Conference (APMC), Kuala Lumpur, Malaysia. He is a Potential Reviewer of many journals and conferences, such as IEEE Access, IEEE Transactions on Circuits and Systems—II: Express Briefs, IEEE Transactions on Electromagnetic Compatibility, *Electronics Letters*, *Microwave and Optical Technology Letters*, *International Journal of RF and Microwave Computer-Aided Engineering*, *Radioengineering*, *PIER Journals*, *Wireless Personal Communications*, and EuCAP Conferences.

NAVEEN MISHRA was born in Deoria, India, in 1990. He received the B.Tech. degree in electronics and communication engineering from Uttar Pradesh Technical University, Lucknow, in 2010, and the Ph.D. degree from the Department of Electronics Engineering, IIT (Indian School of Mines) Dhanbad, India. He joined the Department of Electronics Engineering, IIT (Indian School of Mines) Dhanbad, in January 2014, as a Junior Research Fellow, where he was a Senior Research Fellow, from January 2016 to April 2019. He is currently an Assistant Professor with the Department of Electronics Engineering, School of Electronics Engineering, Vellore Institute of Technology (VIT), Vellore, Tamilnadu, India. He joined VIT University, in May 2019. He has authored or coauthored more than 30 peer-reviewed international/national journal/conference research papers. His current research interests include metamaterial structures and their various applications. He is a Potential Reviewer of many journals and conferences, such as the IEEE Access, IEEE Open Journal of Antennas and Propagation, *Progress in Electromagnetic Research*, and *International Journal of RF and Microwave Computer-Aided Engineering*.

PRASHANT KUMAR SINGH received the B.Tech. degree in electronics and telecommunication engineering from the College of Engineering Roorkee, India, in 2007, the M.E. degree in wireless communication from the Birla Institute of Technology (BIT), Mesra, Ranchi, India, in 2012, and the Ph.D. degree from the Department of Electronics and Communication Engineering, BIT Mesra, in 2018. He has been an Assistant Professor with the Department of Electronics and Communication Engineering, Birsa Institute of Technology Sindri, Jharkhand, India, since December 2022. He served as an Associate Professor with the University College of Engineering and Technology (UCET), Hazaribag, India, and an Assistant Professor with the Department of Electronics and Communication Engineering, National Institute of Science and Technology (NIST), Berhampur, India. He has authored or coauthored more than 20 peer-reviewed journals/conference papers/patents/book chapters. His current research interests include microwave- and millimeter-wave filters, antennas, sensors, and THz systems. He is a Potential Reviewer of various journals, such as *PIER Journals*, *Microwave and Optical Technology Letters*, and *International Journal of RF and Microwave Computer-Aided Engineering*.

ANAND SHARMA (Member, IEEE) was born in Agra, Uttar Pradesh, India, in 1990. He received the B.Tech. degree in electronics and communication engineering from Uttar Pradesh Technical University, Lucknow, India, in 2012, the M.Tech. degree in electronics and communication engineering from the Jaypee University of Engineering and Technology, Guna, Madhya Pradesh, India, and the Ph.D. degree from the Department of Electronics Engineering, Indian Institute of Technology (Indian School of Mines) Dhanbad, India, in 2018. He is currently an Assistant Professor with the Department of Electronics and Communication Engineering, Motilal Nehru National Institute of Technology Allahabad, Prayagraj, Uttar Pradesh. He has authored or coauthored more than 80 research papers in international/national journals/conference proceedings. His research interests include dielectric resonator antennas and microstrip antennas.